Expert Systems with Applications 39 (2012) 11156–11163

Contents lists available at SciVerse ScienceDirect

Expert Systems with Applications

journal homepage: www.elsevier.com/locate/eswa

Fractal analysis features for weak and single-channel upper-limb EMG signals

Angkoon Phinyomark *, Pornchai Phukpattaranont, Chusak Limsakul

Department of Electrical Engineering, Faculty of Engineering, Prince of Songkla University, 15 Kanjanavanich Road, Kho Hong, Hat Yai, 90112 Songkhla, Thailand

ARTICLE INFO

Keywords:
Electromyography signal
Human–computer interface
Multifunction myoelectric control system
Detrended fluctuation analysis
Low-level movements
Robustness
Surface electrodes

ABSTRACT

Electromyography (EMG) signals are the electrical manifestations of muscle contractions. EMG signals may be weak or at a low level when there is only a small movement in the major corresponding muscle group or when there is a strong movement in the minor corresponding muscle group. Moreover, in a single-channel EMG classification identifying the signals may be difficult. However, weak and single-channel EMG control systems offer a very convenient way of controlling human–computer interfaces (HCIs). Identifying upper-limb movements using a single-channel surface EMG also has a number of rehabilitation and HCI applications. The fractal analysis method, known as detrended fluctuation analysis (DFA), has been suggested for the identification of low-level muscle activations. This study found that DFA performs better in the classification of EMG signals from bifunctional movements of low-level and equal power as compared to other successful and commonly used features based on magnitude and other fractal techniques.

1. Introduction

Electromyography (EMG) or myoelectric signals are an electrical potential generated by the muscles. Normally, EMG signals can be measured by either an invasive method using a needle electrode sensor or a non-invasive method using a surface electrode sensor. More clinical skill is needed to deploy needle electrodes and they can cause pain for the user, whereas surface electrodes can be easily applied and still provide important information for use in many applications (Merletti & Hermens, 2004; Pandey & Mishra, 2009).

Prosthetic controls and a number of other rehabilitation and human computer interface (HCI) applications (Alkan & Günay, 2012; Du, Lin, Shyu, & Chen, 2010; Rafiee, Rafiee, Yavari, & Schoen, 2011) require the automated identification of upper-limb movements, and surface EMG signals are one of the most useful methods of determining a movement by estimating the strength of associated muscle contractions based on the electrical activity of the muscles. Therefore, EMG-based controls are favored in many HCI applications. These control systems are normally referred to as "myoelectric control systems" or "MCSs" (Oskoei & Hu, 2007) and their main applications are in prosthetic control (Zecca, Micera, Carrozza, & Dario, 2002) and power-assisted wheelchair control (Phinyomark, Phukpattaranont, & Limsakul, 2011).

However, the classification of actions associated with EMG signals for multifunction MCSs is not simple when there are a number of simultaneously active muscles and when the muscle activity is weak (Arjunan, 2008; Arjunan & Kumar, 2010; Maitrot, Lucas, Doncarli, & Farina, 2005; Naik, Kumar, & Arjunan, 2009, 2010; Singh & Kumar, 2008). Such cases cannot be avoided if EMG is used to identify many complex actions through a single EMG channel. This paper will firstly examine why the classification of low-level muscle activations with a single EMG channel is important, and secondly, how this could be of benefit in multifunction MCSs.

In order to increase the number of control commands, complex actions are commonly included in classification systems (Englehart, Hudgin, & Parker, 2001; Geethanjali & Ray, 2011; Hudgins, Parker, & Scott, 1993; Kim, Choi, Moon, & Mun, 2011). However, a number of muscles are simultaneously active when dynamic and/or complex movements are performed. Therefore, most studies of multifunction MCSs (Du et al., 2010; Englehart et al., 2001; Geethanjali & Ray, 2011; Oskoei & Hu, 2007; Phinyomark et al., 2011) have employed multi-channel sensors to deal with the problems arising from this and to increase the classification performance. However, increasing the number of surface electrode sensors in a system increases its complexity and the computational time needed to classify actions, and also represents an inconvenience to the user (Hudgins et al., 1993; Parker, Englehart, & Hudgins, 2004). So the use of a single electrode-sensor channel is beneficial because it does not require much expertise to fix the electrode positions and also has the further advantages of lower cost and lower computational complexity. Moreover, it is generally a more convenient method for users to control prostheses and other HCIs.

Recent research has reported on the use of single electrode-sensor channel surface EMG signals (Arjunan, 2008; Arjunan & Kumar, 2010; Maitrot et al., 2005; Singh & Kumar, 2008) rather than using multi-channel sensors. However, this entails the problem that when using EMG to identify dynamic and/or complex actions it is

* Corresponding author. Tel.: +66 (0) 74 55 8831; fax: +66 (0) 74 45 9395.
E-mail address: angkoon.p@hotmail.com (A. Phinyomark).

0957-4174/$ - see front matter © 2012 Elsevier Ltd. All rights reserved.
http://dx.doi.org/10.1016/j.eswa.2012.03.039

necessary to map the EMG signals corresponding to the contractions of different muscles (Duchêne & Goubel, 1993; Gazzoni, Farina, & Merletti, 2004). Generally, the ability of EMG to classify movements is based on information obtained from different muscle positions and also on the information contained in features of the signal. Where the information obtained from the muscles is limited to a single channel, the ability of the feature extraction method needs to be increased to compensate for the loss of signal detection sources (Parker et al., 2004). In recent studies (Arjunan, 2008; Arjunan & Kumar, 2010; Maitrot et al., 2005; Singh & Kumar, 2008), time-scale based features (i.e., discrete wavelet transform or DWT, and wavelet packet transform or WPT) and fractal-based features (i.e., Higuchi's fractal dimension or HFD) have been used instead of features based on magnitude techniques (e.g., root mean square, mean absolute value, waveform length and zero crossing) that require an array of electrodes (Crawford, Miller, Shenoy, & Rao, 2005; Nagata, Adno, Magatani, & Yamada, 2005) and a high level of EMG signal (Naik et al., 2010; Zardoshti-Kermani, Wheeler, Badie, & Hashemi, 1995).

Another important limitation of single channel-based control (Arjunan, 2008; Arjunan & Kumar, 2010; Maitrot et al., 2005; Singh & Kumar, 2008) is that there is no single muscle that has a major correspondence to many kinds of movement (Parker et al., 2004). So the signals derived from one of a selected group of muscles will contain both high-level and low-level EMG signals even when strong movements are performed. Arjunan (2008) defined EMG signals as being at low-level or weak, when "there is a little movement in the major corresponding muscle group". In order to cover all possible definitions of low level EMG signals, this study will also take consideration of the alternative definition: there is a strong movement in the minor corresponding muscle group.

Generally, magnitude and/or statistical features, which are the most successful and commonly used features, are unreliable at low-levels of muscle contraction or with those that possess equal energy value (Naik et al., 2010). This is because the relationship between EMG and contraction force is not linear at low-levels of EMG signal (Basmajian & De Luca, 1985; Kleine, van Dijk, Lapatki, Zwarts, & Stegeman, 2007) and at low-levels of contraction, the signal-to-noise ratio (SNR) for EMG is very poor (Arjunan & Kumar, 2010; Naik et al., 2010; Tkach, Huang, & Kuiken, 2010). As a result, it is difficult to automatically distinguish the EMG activity from the background activity or noise by using features based on magnitude techniques (Gazzoni et al., 2004). On the other hand, time-scale based features have more computational complexity and are more time consuming and cannot be related to low-level muscle activity, without manual supervision (Arjunan, 2008).

In order to determine the reliable features of low-level muscle activations, a feature set needs to be extracted from EMG, which interprets the complex properties of the muscle during activity, instead of a feature set interpreting the strength of the muscle contraction. To overcome both the limitations inherent in the use of a single-channel sensor and in low-level EMG, this study examined the use of an advanced fractal analysis technique, called detrended fluctuation analysis (DFA) (Peng, Havlin, Stanley, & Goldberger, 1995), to classify low-level EMG signals derived from a single surface-electrode channel for bifunctional commands. (It should be noted that a bifunctional movement is a pair of actions, such as flexion-extension, occurring about a transverse axis through a joint). DFA was computed in the time domain (Peng et al., 1995) and thereby avoided the effect of noise trends (Hu, Ivanov, Chen, Carpena, & Stanley, 2001). In this way, it was able to offer better performance in the case of low-level activity classification than other successful fractal EMG techniques, such as HFD (Arjunan, 2008; Arjunan & Kumar, 2010). In addition, it could usefully be combined with other methods, which are successful in the classification of high-level EMG signals, for multifunction MCSs.

2. Theory

A number of studies have established that EMG signals are non-linear and non-stationary (only short-term stationary) (Lei, Wang, & Feng, 2001; Meng, Liu, & Liu, 2005), and the fractal dimension (FD) has been used as a measure of the non-linear property in EMG signals. In addition, FD is related to the muscle size and complexity and not to the strength of the muscle contraction (Arjunan, 2008; Arjunan & Kumar, 2010; Lei et al., 2001; Meng et al., 2005). Therefore, in the recent past, a number of FD methods (i.e., HFD, Katz's FD, and the box-counting method) have been proposed for the classification of EMG signals (Gitter & Czerniecki, 1995; Gupta, Suryanarayanan, & Reddy, 1997; Xu & Xiao, 1997). However, these FD methods have their own disadvantages which have been discussed in previous work by the present authors (Phinyomark, Phothisonothai, Limsakul, & Phukpattaranont, 2009; Phinyomark, Phukpattaranont, Limsakul, & Phothisonothai, 2011). On the other hand, DFA has been established as one of the most generally useful EMG techniques, successfully classifying eight upper-limb movements from five muscles (Phinyomark et al., 2011) as well as one of the most robust (Phinyomark, Phothisonothai, Limsakul, & Phukpattaranont, 2010).

2.1. Detrended fluctuation analysis

DFA is one of the most frequently used fractal time-series algorithms and was first introduced by Peng et al. (1995). The scaling exponent determined by DFA has proved to be a useful parameter in many applications during the last two decades, notably in earthquake time series, tree-ring width time series, image texture analysis (Alvarez-Ramirez, Rodriguez, Cervantes, & Echeverria, 2006; Telesca & Lovallo, 2010; Telesca, Lovallo, Lapenna, & Macchiato, 2008; Telesca, Lovallo, Ramirez-Rojas, & Angulo-Brown, 2009) and complex electro-physiological signals: EEG (electroencephalography) and ECG (electrocardiography) (Jospin et al., 2007; Rodriguez, Lerma, Echeverria, & Alvarez-Ramirez, 2008). The advantages of DFA are that it combines the benefits of features from both the time domain and the time-frequency domain. In addition, DFA offers the advantage over the time-scale domain methods, DWT and WPT, that its performance does not rely on the selection of wavelet basis functions (Phinyomark, Limsakul, & Phukpattaranont, 2010), instead exploiting the non-stationary property of EMG signals and thus achieving computational simplicity. For this reason, the scaling exponent obtained from DFA was used as the main feature in this study.

DFA is a modified root mean square analysis of a random walk (RW): a mathematical representation of a trajectory based on a succession of random steps (Peng et al., 1995). To illustrate the DFA procedure Fig. 1(a) shows the surface EMG time series. This is denoted by $\{x(t)\}$, where t is the discrete time in the range $[1, N]$ and N is the sample length of the time series. The scheme of DFA follows five steps described below:

(1) First, the EMG time series are integrated. This integration process converts the EMG signal into RW. The integrated series, also called profile $y(k)$, is defined by:

$$y(k) = \sum_{t=1}^{k} \left[\{x(t)\} - \overline{x(t)} \right], \quad k = 1, \ldots, N, \tag{1}$$

where $\overline{x(t)}$ represents the average value of $x(t)$. The result based on the example in Fig. 1(a) is shown in Fig. 1(b) with fluctuating gray solid lines.

(2) The profiles are divided into L equal-size boxes as shown in Fig. 1(b) with vertical dashed lines. Each box has an n time point, where n is defined as the largest integer not greater than N divided by L. In practice, the minimum box size n_{min}

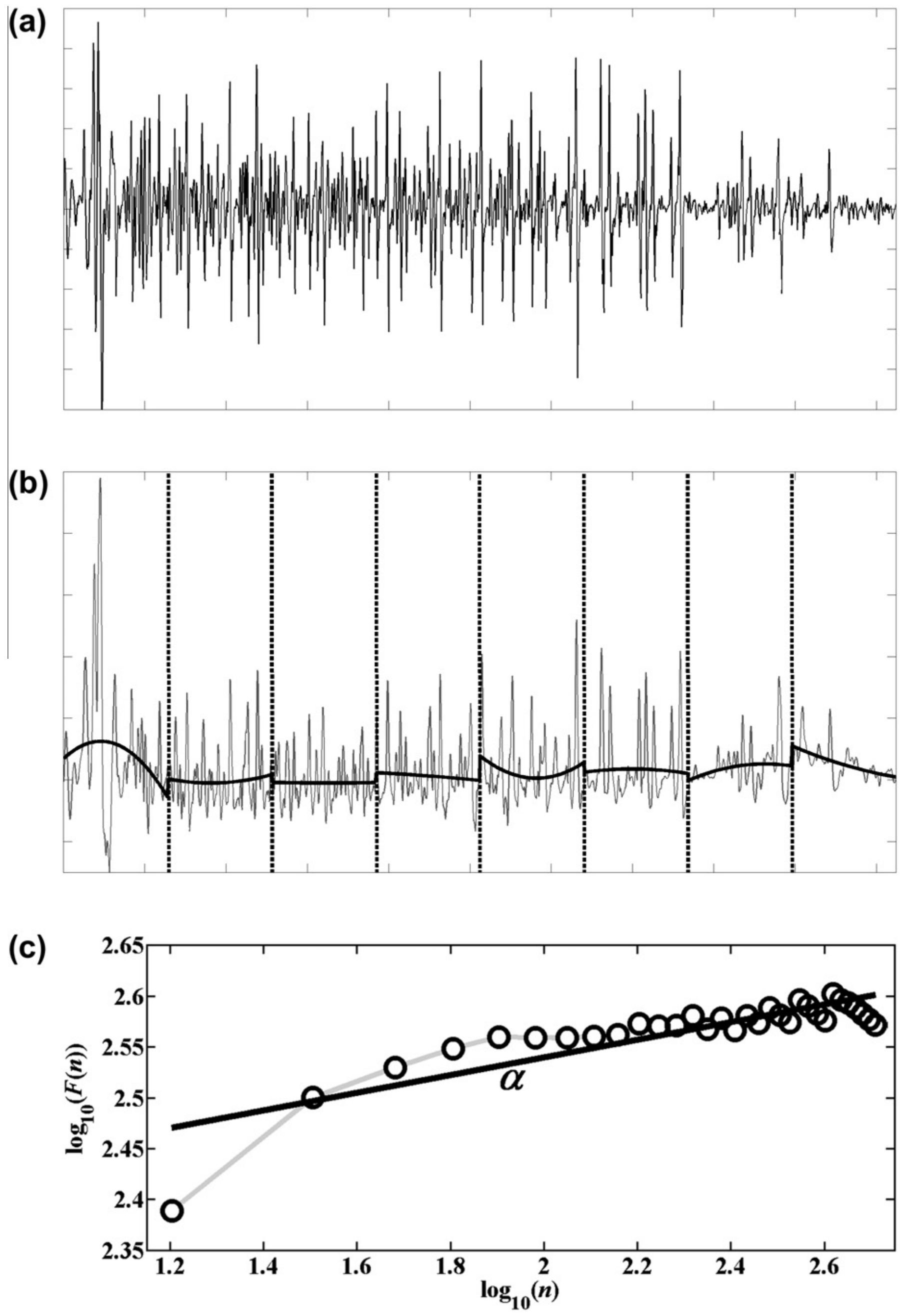

Fig. 1. The procedure of the DFA method (a) the raw EMG time series of a movement (b) the integrated series with different box sizes n (c) the log-log representation where distribution of the corresponding points characterizes the fluctuations in the surface EMG signal. The slope α represents the scaling exponent.

is approximately four, the maximum box size n_{max} is one-tenth of the signal length ($N/10$) and the box size increment is based on a power of two (Phinyomark et al., 2011).

(3) Within each box size n, a least-square fit is applied to the profiles $\{y(k)\}$ as shown in Fig. 1(b) with black solid curves. The y coordinate of the fitted function within the time window is denoted by $y_n(k)$. Each least-square line presents the semi-local trend in that window. In practice, the quadratic polynomial fit is used.

(4) The RMS fluctuation of the profiles and the detrended time series is calculated by:

$$F(n) = \sqrt{\frac{1}{N}\sum_{k=1}^{N}[y(k) - y_n(k)]^2}. \tag{2}$$

(5) The computation is repeated over the all the box sizes, as set out in step 2.

As a result, the linear relationship between $F(n)$ and n is plotted in a log-log graph. The slope of the line relating $\log(F(n))$ to $\log(n)$ characterizes the fluctuation which is shown in Fig. 1(c). This slope indicates the presence of the power law (fractal) scaling known as the DFA scaling exponent, α (Alpha) which is used as a feature parameter in this study.

The self-similarity parameter α calculated as:

$$\alpha = \frac{[\Delta\log_{10}(F(n))]}{[\Delta\log_{10}(n)]}. \tag{3}$$

The scaling exponents estimated by DFA lie between 0 and 2 (Gao et al., 2006; Peng et al., 1995). A larger value of the scale exponent α represents a smaller FD.

2.2. Other conventional feature methods

To verify the ability of DFA, its abilities need to be compared with other established EMG features of which the root mean square (RMS), the waveform length (WL), the maximum fractal length (MFL) and the HFD are the four considered in this paper. The first three features are calculated in the time domain based on amplitude value. The most commonly used method used in EMG signal analysis in both clinical and engineering applications is RMS (Hudgins et al., 1993; Naik et al., 2010; Oskoei & Hu, 2007; Parker et al., 2004; Tkach et al., 2010; Zardoshti-Kermani et al., 1995; Zecca et al., 2002) modeled as an amplitude modulated Gaussian random process applied to constant force and non-fatiguing contractions. WL is also popular and has proved to be the best option in a number of studies (Oskoei & Hu, 2008; Phinyomark, Hirunviriya, Limsakul, & Phukpattaranont, 2010) when used as a single feature for EMG signal classification, performing best in accuracy, stability and computation cost. MFL is a recently established method for measuring low-level muscle activation (Arjunan, 2008; Arjunan & Kumar, 2010). When the smallest scale is set to one, the definition of MFL resembles a modified version of WL by using the RMS and logarithm functions. The definitions of the first three time-domain features are expressed respectively as follows:

$$\mathrm{RMS} = \sqrt{\frac{1}{N}\sum_{t=1}^{N} x(t)^2}, \tag{4}$$

$$\mathrm{WL} = \sum_{n=1}^{N-1} |x(n+1) - x(n)|, \tag{5}$$

$$\mathrm{MFL} = \log_{10}\left(\sqrt{\sum_{n=1}^{N-1} (x(n+1) - x(n))^2}\right). \tag{6}$$

Finally, HFD, is one of the most popular fractal time-series algorithms. Like DFA, it is a fractal method and has showed better performance than other fractal methods in the study conducted by Esteller, Vachtsevanos, Echauz, and Litt (2001), and has also shown good performance in the classification of EMG signals (Arjunan, 2008; Arjunan & Kumar, 2010).

Given a finite EMG time series $x = \{x(1), x(2), ..., x(N)\}$, a new k EMG time series X_m^k can be constructed by the following equation:

$$X_m^k = \left\{x(m), x(m+k), x(m+2k), ..., x\left(m + \left\lfloor \frac{N-m}{k} \right\rfloor \cdot k\right)\right\}, \tag{7}$$

where both k and m are integers, and $\lfloor\bullet\rfloor$ is the integer part of $\bullet$. k indicates the discrete time interval between points, whereas $m = 1, 2, \ldots, k$, and m represents the initial time value.

The length of each curve, $L_m(k)$, is then calculated and defined as follow:

$$L_m(k) = \frac{1}{k}\left\{\left(\sum_{i=1}^{\lfloor\frac{N-m}{k}\rfloor} |x(m+ik) - x(m+(i-1)\cdot k)|\right) \cdot \frac{N-1}{\lfloor\frac{N-m}{k}\rfloor \cdot k}\right\}. \tag{8}$$

Then the length of the curve for the time interval k is defined as the average of the m curves $L_m(k)$, for $m = 1, 2, \ldots, k$. Finally, the relationship of this method is $L(k) \propto k^D$. As a result, the linear relationship between $L(k)$ and k is plotted in a log-log graph. The negative slope of the line relating $\log(L(k))$ to $\log(k)$ gives the estimate of the HFD. Based on the findings of Phothisonothai and Nakagawa (2007), in the present study the value of k_{max} was set at 2^7 or 128.

3. Material and methods

3.1. EMG data acquisitions

Experiments were conducted to evaluate the performance of the proposed method to identify different upper-limb activities from surface EMG recorded on the forearm and upper-arm, particularly for low-level muscle activation. Twenty healthy subjects (10 males and 10 females) volunteered to participate in this study. Their mean age was 21.35 (σ = 0.88) years; their mean weight 54.90 (σ = 8.90) kg; and their mean height 163.75 (σ = 7.89) cm. All the subjects were dexterous with their right hands.

Five useful muscle positions on the right arm (4 forearm muscles and 1 upper-arm muscle) were selected. These were: extensor carpi radialis longus muscle (C1), extensor carpi ulnaris muscle (C2), extensor digitorum communis muscle (C3), flexor carpi radialis muscle (C4), and biceps brachii muscle (C5), as shown in Fig. 2(a). EMG data were collected from the five channels using bipolar Ag/AgCl electrodes (H124SG, Kendal ARBO). Five pairs of disposable pre-gelled self-adhesive surface electrodes of 24.0 mm diameter (circular) were applied to the subjects at an inter-electrode distance of 20.0 mm after suitable preparation of the skin with alcohol. An Ag/AgCl electrode (Red Dot 2223, 3 M Health Care) was placed on the wrist to provide a common ground reference. This was also a disposable pre-gelled self-adhesive surface electrode but its diameter was 43.1 mm. The EMG data were amplified and sampled by a commercial wireless EMG measurement system (Mobi6-6b, TMS International B.V.). The signals were amplified with a gain of 19.5x and bandwidths of 20 Hz to 500 Hz. Data were sampled at 1024 Hz with a high resolution of 24 bits.

The EMG data were collected as the volunteers performed eight commonly used, distinct upper-limb movements including forearm pronation (M1), forearm supination (M2), wrist extension (M3), wrist flexion (M4), wrist radial deviation (M5), wrist ulnar deviation (M6), hand open (M7), and hand closed (M8) as shown in Fig. 2(b). These movements have been frequently used in MCS studies (Englehart et al., 2001; Hudgins et al., 1993; Oskoei & Hu, 2007; Parker et al., 2004; Tkach et al., 2010; Zardoshti-Kermani et al., 1995; Zecca et al., 2002). Within each trial, the subject maintained each movement for 2 seconds in duration and separated each movement by a 2-second period in the rest state (R) to avoid any transitional stage (i.e., during movement changes). Moreover, 13-second rest periods were also allowed at the start and the end of each trial to give the subject some preparation time and to avoid any incomplete recording of data due to a cut-off before an action was finished. Thus each trial lasted for a period of 56 seconds. In order to study the fluctuation in the EMG signals, on each of four days, each subject completed 3 sessions, with 5 trials in each session. The order of movements was randomized in each session and an example of the order of movements is shown in Fig. 3. In total, 60 datasets with a duration of 2 seconds were collected for each movement from each subject. Before processing the data, however, all data relating to rest states were removed before the data was extracted so that each trial comprised 16 seconds or 16,384 samples in length.

3.2. Evaluating the functions

After the EMG data were entirely recorded, the power of the EMG signals was computed in order to determine the level of muscle activities. Two categories of four bifunctional movements were defined by power-based criteria: low/high level and equal/unequal power. The four bifunctional movements were: forearm pronation-supination (M1–M2), wrist extension-flexion (M3–M4), wrist radial-ulnar deviation (M5–M6), and hand open-closed (M7-M8).

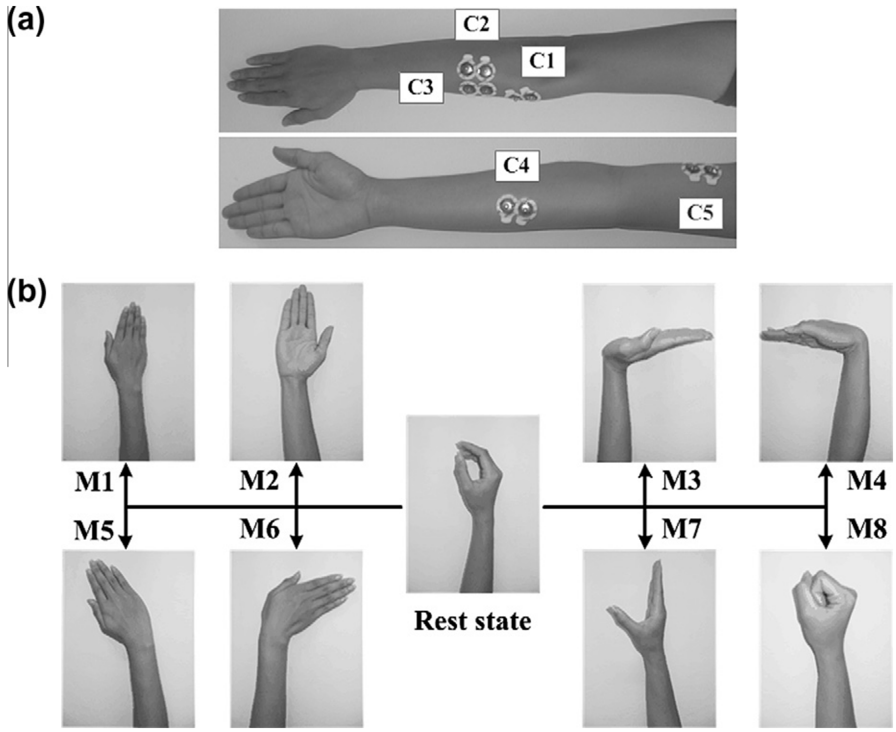

Fig. 2. (a) Five muscle channels on the right arm (four channels on the forearm and one channel on the upper-arm). (b) Eight upper-limb movements and rest state.

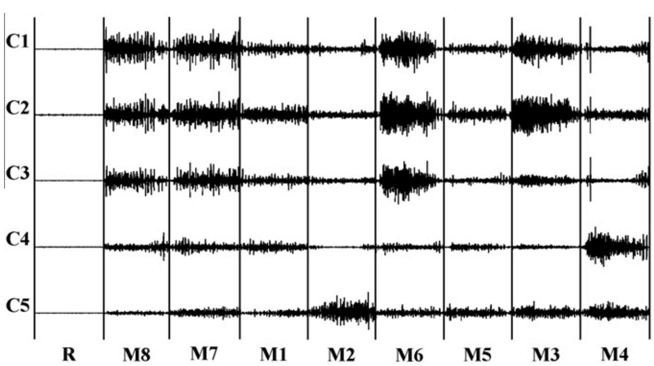

Fig. 3. Five-channel surface EMG signals from eight upper-limb movements and in the rest state in the time domain. Sample from subject 1.

For the first category of movements there were two levels of muscle activation: low and high. In this study, a movement which had a power value lower than or equal to 5000 $(\mu V)^2$ was defined as a low-level EMG signal. Conversely, a high-level EMG signal was defined as one with a power value higher than 5000 $(\mu V)^2$. The value of 5000 $(\mu V)^2$ effectively separated the two levels of EMG signals, since it was observed that a low-level of muscle activity had a maximum voluntary contraction (MVC: a measure of strength when the subjects performed the maximum voluntary wrist extension contraction) level below approximately 25% and this level (25% of MVC) accorded with effort protocols defined in previous studies (Smith & Newham, 2007; Tkach et al., 2010; Zhou et al., 2007).

It should be mentioned that in the second category of bifunctional movements, there were either equal or unequal power types. A movement was defined as equal when the difference of its paired power values was less than 1000 $(\mu V)^2$, a value derived from the standard deviation of the EMG power which was usually equal to or higher than 1000 $(\mu V)^2$. Thus, if the difference in power value was less than 1000 $(\mu V)^2$, it could have been the same movement, or have had an equal EMG power.

Subsequently, the signal-to-noise ratios (SNRs) of all the low-level bifunctional movements which had equal power values were calculated in order to quantify how much of the signal had been corrupted by noise.

Next, the proposed DFA feature and the other four EMG features (RMS, WL, MFL, and HFD) were calculated for each movement, channel and subject. Thereafter, the classification of possible combinations of each bifunctional movement and feature was computed. In order to evaluate the ability of class separability criteria, the classification accuracy of each set was also examined. The Linear discriminant analysis (LDA) classifier was selected to be used due to its high performance in classification, together with its robustness in long-term use and its low computational cost (Englehart et al., 2001; Kaufmann, Englehart, & Platzner, 2010). The LDA was performed by a 10-fold cross validation of each subject and the classification accuracy was computed as an average accuracy based on the results from cross validation testing of all twenty subjects.

Each feature only provided one feature per channel, which was small enough to be combined with other features without adding significantly to the computational burden, but provided a more powerful feature vector. Hudgins et al. (1993) combined several magnitude features into one feature vector, which had comparable performance to several spectral approaches. In this study, eight combinations from five individual features were used to make up the feature-sets. These were: (S1) WL and MFL; (S2) DFA and HFD; (S3) DFA and MFL; (S4) HFD and MFL; (S5) DFA and WL; (S6) HFD and WL; (S7) DFA, MFL, and RMS; and (S8) All features: DFA, HFD, RMS, WL and MFL. The first two groups, S1 and S2, were obtained from similar approaches; magnitude and fractal analysis, respectively. The multi-feature sets S3, S4, S5 and S6 were combinations of magnitude-based features and fractal-based features. Moreover, the multi-feature sets S1-S6 provided a two-dimension feature vector from the single channel. Multiple-feature sets S7 and S8 combined, respectively all the magnitude-based features

Table 1
Average power of each movement of two-second duration and muscle position from 20 subjects (Unit: $(\mu V)^2$. Note that bold and italic numbers are low-level and equal power movements).

Movements	Muscle positions				
	C1	C2	C3	C4	C5
M1	***2060***	6180	***5062***	3470	853
M2	***1845***	4882	***4273***	835	5879
M3	10,329	25,066	21,715	1430	2100
M4	1305	5131	2542	12,437	5950
M5	1330	10,889	3268	***4544***	***2327***
M6	7496	9801	12,232	***4073***	***2606***
M7	3719	11,390	8462	2476	1849
M8	10,861	7241	8585	5251	3169

and all the evaluated features in the study. Their dimensions were 3 for S7 and 5 for S8. Combinations of more than one muscle channel however, were beyond the scope of this study.

4. Results and discussion

Fig. 3 shows a sample of the surface EMG signals from five muscle positions during eight upper limb movements and the rest state. As can be clearly observed, based on the clean rest-state responses, the raw EMG signals in this study were not greatly contaminated by any kinds of noise such as movement artifacts, power-line interference or electrical noise from electronic equipment. The average power parameters of the eight movements (M1–M8) and five muscle channels (C1–C5) were calculated as shown in Table 1. The bifunctional movements which are defined as being of the equal power type are M1–M2 with C1, M1–M2 with C3, M5–M6 with C4, M5–M6 with C5, and M7–M8 with C3. However, only the first four combinations were determined to be low-level movements since the final combination exceeded the study's definition of high-level muscle activation. Therefore, the EMG data from the first four combination movements were employed as the candidate data in this study. The profile of these signals is shown in Fig. 4 together with their SNRs, which can also be used to confirm the equal power types of these signals. Moreover, it can be observed that all the SNRs are higher than 24 dB. This means that these low-level signals were definitely not noise.

The average classification accuracies and standard deviations of the five single-features for each bifunctional movement and muscle position from the 20 subjects are shown in Table 2. From this table, it can be seen that when the difference between the powers of the bifunctional movements had a large value, the features based on magnitude analysis (RMS, WL and MFL) performed better than the features based on fractal analysis (DFA and HFD). However, in some cases DFA performed better in class separability than the magnitude features in the combination of channel C2 with movements M7–M8, and performed equally well in class separability with the magnitude features in the combination of C1 with M7–M8 and of C2 with M3–M4.

On the other hand, when the difference between the powers of the bifunctional movements was small, DFA performed better than other features, including MFL which has been established as a successful means of measuring low level muscle activation (Arjunan & Kumar, 2010), except in the combination of M7-M8 with C3 which was determined to be a high-level contraction. Clearly therefore, MFL is not suitable for low-level muscle activations with small power value differences, whereas DFA does not suffer from this problem when quantifying the suitability of the feature space, as highlighted in Table 2 where figures relating to low-level and equal power movements are italicised and highlighted in bold. In addition, DFA also performed better than HFD which extracts feature based on fractal analysis.

Based on the average classification accuracy across the four bifunctional movements and five features, muscle position C2 shows the highest accuracy at 77.57%, followed closely by muscle position C4 at 77.12%. On the other hand, muscle position C5 has the lowest accuracy at 69.65%. Based on only these five-muscles, muscle position C2 is recommended to be used as a single EMG channel. However, if a two-EMG channel system is adopted, then a combination of muscle positions C2 and C4 may give useful EMG information based on both extensor and flexor muscles.

Nevertheless, the performance of EMG signal classification with only one feature and one sensor is not sufficient for practical purposes, particularly when low-level and equal-power EMG signals are used. To enhance the performance of the EMG recognition system, a multi-feature system should be used. In this study, eight multi-feature sets were evaluated. The average classification accuracies and the standard deviations of all the multiple-feature sets are shown in Table 3. Multi-feature sets S1 and S2 were obtained from similar approaches; magnitude and fractal analysis, respectively. Their accuracies were slightly greater than those obtained from single features. Multi-feature sets S3, S4, S5 and S6 were combinations of magnitude-based features and fractal-based features. From Table 3 it can be seen that from multi-feature sets S3, S4, S5 and S6, only sets S3 and S5 exhibited high average accuracy. The accuracy using the combination of DFA and WL/MFL from a single channel was even better than the combination of HFD and MFL that has been previously reported as being used in low-level

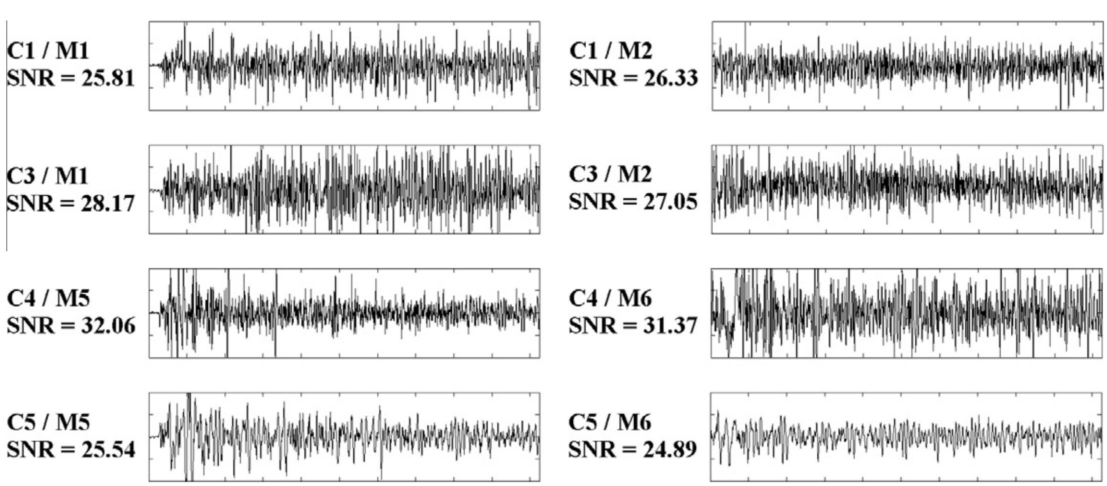

Fig. 4. EMG signals from low-level muscle activity with their SNRs (dB). Note that the minimum and maximum values of the y-axis are -100 and 100 μV.

Table 2
Average classification accuracy (and standard deviation) of five single features from each bifunctional movement and muscle position from 20 subjects (Unit: %. Note that bold and italic numbers are low-level and equal power movements).

Muscle	Feature	Bifunctional movements			
		M1–M2	M3–M4	M5–M6	M7-M8
C1	DFA	***72.42 (12.2)***	79.83 (14.3)	75.75 (13.9)	72.17 (15.4)
	HFD	***70.33 (11.1)***	72.54 (9.8)	63.38 (12.1)	64.63 (10.5)
	RMS	***57.38 (9.0)***	89.67 (10.6)	88.50 (11.4)	72.96 (14.6)
	WL	***56.42 (11.5)***	93.71 (7.3)	85.25 (15.3)	73.29 (13.5)
	MFL	***55.63 (11.6)***	94.63 (8.6)	86.63 (15.2)	75.54 (15.9)
C2	DFA	64.21 (11.7)	93.58 (7.4)	75.50 (18.6)	82.54 (13.9)
	HFD	60.25 (8.4)	79.71 (13.3)	58.96 (11.4)	69.38 (13.0)
	RMS	65.50 (11.5)	92.33 (8.4)	82.75 (15.2)	73.50 (16.5)
	WL	66.83 (11.0)	94.58 (5.8)	82.71 (17.2)	80.33 (14.3)
	MFL	67.71 (10.9)	94.92 (5.3)	83.54 (15.5)	79.83 (14.9)
C3	DFA	***64.46 (12.6)***	85.79 (12.4)	78.33 (14.3)	72.29 (15.8)
	HFD	***63.46 (11.5)***	75.58 (14.2)	63.17 (11.8)	66.58 (10.2)
	RMS	***63.96 (12.0)***	87.42 (12.7)	87.13 (12.6)	75.75 (16.0)
	WL	***61.92 (13.6)***	92.29 (6.8)	88.50 (12.2)	79.54 (15.7)
	MFL	***61.42 (12.2)***	93.13 (8.0)	89.58 (10.8)	80.63 (13.7)
C4	DFA	71.25 (11.7)	79.08 (14.9)	***77.83 (11.0)***	68.75 (14.0)
	HFD	66.71 (9.9)	73.75 (10.0)	***72.33 (11.0)***	63.13 (11.6)
	RMS	83.75 (13.0)	92.71 (8.2)	***73.13 (15.8)***	69.71 (18.5)
	WL	87.67 (10.7)	94.13 (7.9)	***72.42 (14.7)***	74.29 (15.0)
	MFL	88.92 (10.8)	93.38 (12.4)	***72.58 (15.9)***	74.25 (15.8)
C5	DFA	73.58 (15.4)	63.25 (14.5)	***77.42 (15.3)***	56.13 (7.7)
	HFD	68.17 (12.9)	58.33 (2.5)	***73.50 (16.7)***	56.58 (8.7)
	RMS	79.71 (11.5)	68.58 (12.9)	***67.63 (16.9)***	64.88 (13.5)
	WL	87.58 (11.0)	71.33 (14.8)	***75.33 (16.8)***	69.21 (13.4)
	MFL	75.38 (16.3)	71.08 (15.3)	***77.04 (16.3)***	69.38 (13.4)

Table 3
Average classification accuracy (and standard deviation) of eight multiple features from each bifunctional movements and muscle position from 20 subjects (Unit: %).

Feature sets	Bifunctional movements			
	C1/M1–M2	C3/M1–M2	C4/M5–M6	C5/M5–M6
S1	62.13 (13.4)	66.00 (8.9)	73.54 (15.2)	77.96 (14.1)
S2	76.00 (12.6)	67.46 (14.1)	81.13 (7.8)	79.42 (14.5)
S3	75.08 (12.9)	69.83 (12.4)	86.92 (6.9)	85.58 (12.3)
S4	71.92 (13.1)	68.71 (12.8)	80.17 (12.0)	85.00 (10.0)
S5	76.17 (11.7)	71.21 (12.0)	86.21 (7.4)	85.46 (11.7)
S6	71.75 (13.3)	68.54 (13.1)	80.33 (10.9)	85.00 (10.3)
S7	77.63 (11.8)	72.25 (11.1)	87.50 (6.6)	86.17 (11.9)
S8	80.50 (12.2)	77.71 (9.9)	90.67 (4.8)	87.71 (11.4)

movement classification (Arjunan & Kumar, 2010). Moreover, multi-feature sets S7 (DFA, MFL and RMS) and S8 (all features) showed improved accuracy in the recognition system and even in set S8 which used all the features extracted in this study, the computational time – and hence cost – was still lower than using features based on the frequency and/or time-scale domains.

The results relating to computational time and complexity are not reported in this paper because they have been commented on in detail in previous studies. For instance, the computational times of features based on the time domain (both magnitude and fractal-based techniques) have been demonstrated to be lower than features based on DWT and WPT in the time-scale domain (Boostani & Moradi, 2003; Englehart et al., 2001; Hudgins et al., 1993). For fractal features, the computational time of the DFA method is lower than that of the HFD method (Phothisonothai, & Nakagawa, 2007).

5. Conclusion

This study shows that the DFA of a single-channel surface EMG signal, recorded from the forearm and the upper-arm can be used to accurately identify a set of equal-power bifunctional movements, for instance, forearm pronation-supination and wrist radial-ulnar deviation, even when muscle activity is weak. A comparison of DFA features with other successful features demonstrates that DFA offers an improvement in the discrimination accuracy of upper-limb movements, particularly when the recognition system distinguishes low-level and equal-power EMG signals. This technique is recommended for deployment as a useful augmenting feature to increase the ability of multifunction MCSs, especially when they involve the use of low-level and equal-power activities. The use of DFA features may be suitable for numerous EMG applications such as HCIs for patients, the elderly and amputees who are unable to exert high-level muscle activation and cannot create a big enough difference in power between movements.

Acknowledgements

This work was supported in part by the Thailand Research Fund (TRF) through the Royal Golden Jubilee Ph.D. Program (Grant No. PHD/0110/2550), and in part by NECTEC-PSU Center of Excellence for Rehabilitation Engineering, Faculty of Engineering, Prince of Songkla University.

References

Alkan, A., & Günay, M. (2012). Identification of EMG signals using discriminant analysis and SVM classifier. *Expert Systems with Applications, 39*(1), 44–47.
Alvarez-Ramirez, J., Rodriguez, E., Cervantes, I., & Echeverria, J. C. (2006). Scaling properties of image textures: A detrending fluctuation analysis approach. *Physica A, 361*(2), 677–698.
Arjunan, S. P. (2008). Fractal Features of Surface Electromyogram: A New Measure for Low Level Muscle Activation. Ph.D. Dissertation, RMIT University, Melbourne, Victoria, Australia.
Arjunan, S. P., & Kumar, D. K. (2010). Decoding subtle forearm flexions using fractal features of surface electromyogram from single and multiple sensors. *Journal of NeuroEngineering and Rehabilitation, 7*(53).
Basmajian, J., & De Luca, C. J. (1985). *Muscles alive: Their functions revealed by electromyography*. Baltimore, MD: Williams & Wilkins.

Boostani, R., & Moradi, M. H. (2003). Evaluation of the forearm EMG signal features for the control of a prosthetic hand. *Physiological Measurement, 24*(2), 309–319.

Crawford, B., Miller, K., Shenoy, P., & Rao, R. (2005). *Real-time classification of electromyographic signals for robotic control. Technical Report*. University of Washington.

Du, Y.-C., Lin, C.-H., Shyu, L.-Y., & Chen, T. (2010). Portable hand motion classifier for multi-channel surface electromyography recognition using grey relational analysis. *Expert Systems with Applications, 37*(6), 4283–4291.

Duchêne, J., & Goubel, F. (1993). Surface electromyogram during voluntary contraction: Processing tools and relation to physiological events. *Critical Reviews in Biomedical Engineering, 21*(4), 313–397.

Englehart, K., Hudgin, B., & Parker, P. A. (2001). A wavelet-based continuous classification scheme for multifunction myoelectric control. *IEEE Transactions on Biomedical Engineering, 48*(3), 302–311.

Esteller, R., Vachtsevanos, G., Echauz, J., & Litt, B. (2001). A comparison of waveform fractal dimension algorithms. *IEEE Transactions on Circuits and Systems I: Fundamental Theory and Applications, 48*(2), 177–1831.

Gao, J., Hu, J., Tung, W. W., Cao, Y., Sarshar, N., & Roychowdhury, V. P. (2006). Assessment of lung-range correlation in time series: How to avoid pitfalls. *Physical Review E, 73*(016117).

Gazzoni, M., Farina, D., & Merletti, R. (2004). A new method for the extraction and classification of single motor unit action potentials from surface EMG signals. *Journal of Neuroscience Methods, 136*(2), 165–177.

Geethanjali, P., & Ray, K. K. (2011). Identification of motion from multi-channel EMG signals for control of prosthetic hand. *Australasian Physical and Engineering Science in Medicine, 34*(3), 419–427.

Gitter, J. A., & Czerniecki, M. J. (1995). Fractal analysis of the electromyographic interference pattern. *Journal of Neuroscience Methods, 58*(1–2), 103–108.

Gupta, V., Suryanarayanan, S., & Reddy, N. P. (1997). Fractal analysis of surface EMG signals from the biceps. *International Journal of Medical Informatics, 45*(3), 185–192.

Hu, K., Ivanov, P. Ch., Chen, Z., Carpena, P., & Stanley, H. E. (2001). Effect of trends on detrended fluctuation analysis. *Physical Review E, 64*(011114).

Hudgins, B., Parker, P., & Scott, R. (1993). A new strategy for multifunction myoelectric control. *IEEE Transactions on Biomedical Engineering, 40*(1), 82–94.

Jospin, M., Caminal, P., Jensen, E. W., Litvan, H., Vallverdu, M., Struys, M. M. R. F., et al. (2007). Detrended fluctuation analysis of EEG as a measure of depth of anesthesia. *IEEE Transactions on Biomedical Engineering, 54*(5), 840–846.

Kaufmann, P., Englehart, K., & Platzner, M. (2010). Fluctuating EMG signals: Investigating long-term effects of pattern matching algorithms. In *Proceedings of 32nd annual international conference of the IEEE engineering in medicine and biology society* (pp. 6357–6360).

Kim, K. S., Choi, H. H., Moon, C. S., & Mun, C. W. (2011). Comparison of k-nearest neighbor, quadratic discriminant and linear discriminant analysis in classification of electromyogram signals based on the wrist-motion directions. *Current Applied Physics, 11*(3), 740–745.

Kleine, B. U., van Dijk, J. P., Lapatki, B. G., Zwarts, M. J., & Stegeman, D. F. (2007). Using two-dimensional spatial information in decomposition of surface EMG signals. *Journal of Electromyography and Kinesiology, 17*(5), 535–548.

Lei, M., Wang, Z., & Feng, Z. (2001). Detecting nonlinearity of action surface EMG signal. *Physics Letters A, 290*(5–6), 297–303.

Maitrot, A., Lucas, M.-F., Doncarli, C., & Farina, D. (2005). Signal-dependent wavelets for electromyogram classification. *Medical and Biological Engineering and Computing, 43*(4), 487–492.

Meng, Y., Liu, Y., & Liu, B. (2005). Test nonlinear determinacy of electromyogram. In *Proceedings of 27th annual international conference of the IEEE engineering in medicine and biology society* (pp. 4592–4595).

Merletti, R., & Hermens, H. (2004). Detection and conditioning of the surface EMG signal. In R. Merletti & P. Parker (Eds.), *Electromyography: Physiology, engineering, and noninvasive applications* (pp. 107–132). New Jersey: John Wiley & Sons.

Nagata, K., Adno, K., Magatani, K., & Yamada, M. (2005). A classification method of hand movements using multi channel electrode. In *Proceedings of 27th annual international conference of the IEEE engineering in medicine and biology society* (pp. 2375–2378).

Naik, G. R., Kumar, D. K., & Arjunan, S. (2009). Use of sEMG in identification of low level muscle activities: Features based on ICA and fractal dimension. In *Proceedings of 31st annual international conference of the IEEE engineering in medicine and biology society* (pp. 364–367).

Naik, G. R., Kumar, D. K., & Arjunan, S. P. (2010). Pattern classification of Myo-Electrical signal during different maximum voluntary contractions: A study using BSS techniques. *Measurement Science Review, 9*(1), 1–6.

Oskoei, M. A., & Hu, H. (2007). Myoelectric control systems—A survey". *Biomedical Signal Processing and Control, 2*(4), 275–294.

Oskoei, M. A., & Hu, H. (2008). Support vector machine-based classification scheme for myoelectric control applied to upper limb. *IEEE Transactions on Biomedical Engineering, 55*(8), 1956–1965.

Pandey, B., & Mishra, R. B. (2009). An integrated intelligent computing model for the interpretation of EMG based neuromuscular diseases. *Expert Systems with Applications, 36*(5), 9201–9213.

Parker, P. A., Englehart, K. B., & Hudgins, B. S. (2004). Control of powered upper limb prostheses. In R. Merletti & P. Parker (Eds.), *Electromyography: Physiology, engineering, and noninvasive applications* (pp. 453–476). New Jersey: John Wiley & Sons.

Peng, C. K., Havlin, S., Stanley, H. E., & Goldberger, A. L. (1995). Quantification of scaling exponents and crossover phenomena in nonstationary heartbeat time series. *Chaos, 5*(1), 82–87.

Phinyomark, A., Hirunviriya, S., Limsakul, C., & Phukpattaranont, P. (2010). Evaluation of EMG feature extraction for hand movement recognition based on Euclidean distance and standard deviation. In *Proceedings of 7th international conference on electrical engineering, electronics, computer, telecommunication, and information technology* (pp. 856–860).

Phinyomark, A., Limsakul, C., & Phukpattaranont, P. (2010). Optimal wavelet functions in wavelet denoising for multifunction myoelectric control. *ECTI Transactions on Electrical Engineering, Electronics, Computer, Telecommunication, and Information Technology, 8*(1), 43–52.

Phinyomark, A., Phukpattaranont, P., & Limsakul, C. (2011). A review of control methods for electric power wheelchairs based on electromyography (EMG) signals with special emphasis on pattern recognition. *IETE Technical Review, 28*(4), 316–326.

Phinyomark, A., Phothisonothai, M., Limsakul, C., & Phukpattaranont, P. (2009). Detrended fluctuation analysis of electromyography signal to identify hand movement. In *Proceedings of 2nd biomedical engineering international conference* (pp. 324–329).

Phinyomark, A., Phothisonothai, M., Limsakul, C., & Phukpattaranont, P. (2010). Effect of trends on detrended fluctuation analysis for surface electromyography (EMG) signal. In *Proceedings of 8th PSU-engineering conference* (pp. 333–338).

Phinyomark, A., Phukpattaranont, P., Limsakul, C., & Phothisonothai, M. (2011). Electromyography (EMG) signal classification based on detrended fluctuation analysis. *Fluctuation Noise Letter, 10*(3), 281–301.

Phothisonothai, M., & Nakagawa, M. (2007). Fractal-based EEG data analysis of body parts movement imagery tasks. *Journal of Physiological Sciences, 57*(4), 217–226.

Rafiee, J., Rafiee, M. A., Yavari, F., & Schoen, M. P. (2011). Feature extraction of forearm EMG signals for prosthetics. *Expert Systems with Applications, 38*(4), 4058–4067.

Rodriguez, E., Lerma, C., Echeverria, J. C., & Alvarez-Ramirez, J. (2008). ECG scaling properties of cardiac arrhythmias using detrended fluctuation analysis. *Physiological Measurement, 29*(11), 1255–1266.

Singh, V. P., & Kumar, D. K. (2008). Classification of low-level finger contraction from single channel surface EMG. In *Proceedings of 30th annual international conference of the IEEE engineering in medicine and biology society* (pp. 2900–2903).

Smith, I. C., & Newham, D. J. (2007). Fatigue and functional performance of human biceps muscle following concentric or eccentric contractions. *Journal of Applied Physiology, 102*(1), 207–213.

Telesca, L., & Lovallo, M. (2010). Long-range dependence in tree-ring width time series of Austrocedrus Chilensis revealed by means of the detrended fluctuation analysis. *Physica A, 389*(19), 4096–4104.

Telesca, L., Lovallo, M., Lapenna, V., & Macchiato, M. (2008). Space-magnitude dependent scaling behaviour in seismic interevent series revealed by detrended fluctuation analysis. *Physica A, 387*(14), 3655–3659.

Telesca, L., Lovallo, M., Ramirez-Rojas, A., & Angulo-Brown, F. (2009). Scaling instability in self-potential earthquake-related signals. *Physica A, 388*(7), 1181–1186.

Tkach, D., Huang, H., & Kuiken, T. A. (2010). Study of stability of time-domain features for electromyographic pattern recognition. *Journal of NeuroEngineering and Rehabilitation, 7*(21).

Xu, Z., & Xiao, S. (1997). Fractal dimension of surface EMG and its determinants. In *Proceedings of 19th annual international conference of the IEEE engineering in medicine and biology society* (pp. 1570–1573).

Zardoshti-Kermani, M., Wheeler, B. C., Badie, K., & Hashemi, R. M. (1995). EMG feature evaluation for movement control of upper extremity prostheses. *IEEE Transactions on Rehabilitation Engineering, 3*(4), 324–333.

Zecca, M., Micera, S., Carrozza, M. C., & Dario, P. (2002). Control of multifunctional prosthetic hands by processing the electromyographic signal. *Critical Reviews in Biomedical Engineering, 30*(4–6), 459–485.

Zhou, P., Lowery, M. M., Englehart, K. B., Huang, H., Li, G., Hargrove, L., et al. (2007). Decoding a new neural-machine interface for control of artificial limbs. *Journal of Neurophysiology, 98*(5), 2974–2982.